



CHORUS

This is the accepted manuscript made available via CHORUS. The article has been published as:

Analytical solution and scaling of fluctuations in complex networks traversed by damped, interacting random walkers

Mehdi Bagheri Hamaneh, Jonah Haber, and Yi-Kuo Yu

Phys. Rev. E **92**, 052803 — Published 5 November 2015

DOI: [10.1103/PhysRevE.92.052803](https://doi.org/10.1103/PhysRevE.92.052803)

Analytical Solution and Scaling of Fluctuations in Complex Networks Traversed by Damped, Interacting Random Walkers

Mehdi Bagheri Hamaneh, Jonah Haber, and Yi-Kuo Yu*
National Center for Biotechnology Information, National Library of Medicine,
National Institutes of Health, 8600 Rockville Pike, Bethesda, MD 20894

A general model for random walks (RWs) on networks is proposed. It incorporates damping and time-dependent links, and it includes standard (undamped, noninteracting) RWs (SRWs), coalescing RWs and coalescing-branching RWs as special cases. The exact, time-dependent solutions for the average numbers of visits (w) to nodes and their fluctuations (σ^2) are given, and the long-term σ - w relation is studied. Although $\sigma \propto w^{1/2}$ for SRWs, this power law can be fragile when coalescing-branching interaction is present. Damping, however, often strengthens it but with an exponent generally different from 1/2.

PACS numbers: 89.75.Hc, 89.20.Hh, 89.75.Da

I. INTRODUCTION

Complex networks have diverse applications in biology [1–4], finance [5], traffic [6, 7], the world-wide web [8], social networks [9], *etc.* In these networks, random walks (RWs) are often used as a generic model for the flow of the quantity of interest [2–4, 6, 8]. Two RW models, namely, the standard RW (SRW) and the coalescing RW (CRW), are of particular interest because of their widespread applications. For SRW, its applications are well-known. On the other hand, a specialized version of CRW can be mapped to the voter model [10], which has numerous applications such as spatial conflict [11], diffusion-controlled reaction [12], opinion dynamics [9, 13], population genetics [14], *etc.* In a SRW, non-interacting random walkers (RWers) freely diffuse on the network, whereas in a CRW, RWers reaching a node coalesce into one before moving to the next node. Interestingly, these two seemingly distinct RW models can be treated under one unified framework, because in either model RWers reaching the same node become indistinguishable. Capitalizing on the indistinguishability, we present in this paper a general formalism that covers SRW and CRW as special cases, handles the flow loss (damping) that is prevalent in most networks, and can be applied to networks with time-dependent links. We give the exact solutions for the average number of visits (w_i) to node i and its variance (σ_i^2) at any given time.

Calculating σ with full time-dependence can be useful for many reasons. First, when σ is used to define extreme events [15, 16], its short-time solution is helpful in disaster preparedness. Second, systems with intrinsic time-dependence may never reach equilibrium and require a fully time-dependent solution. For instance, effective disease control requires good estimates of the growth/movement of the infected population and their fluctuations as functions of time. Third, it allows us to broaden the scope of the extensively studied CRW model

to include its long-time σ - w relation, which, to the best of our knowledge, has not yet been explored. This relation, however, has been extensively studied in other context. For example, Menezes and Barabasi [8] studied several real-world networks and found $\sigma \propto w^\alpha$, with α close to either 1/2 or 1. They argued that strong external driving causes $\alpha \approx 1$ and that α can be smaller (still $\geq 1/2$) when the externally induced fluctuations are modest. For a SRW, Meloni *et al.* [17] showed analytically that absent any external force $\alpha = 1/2$ in the stationary regime and that in some cases even a small external drive can result in an α close to 1. Defining w to be the total number of visits to a node multiplied by a power of its degree, Eisler and Kertesz [18] concluded that $0 < \alpha < 1$ even when there is no external driving. Duch and Arenas proposed a model in which, after arriving at a node, noninteracting RWers wait in a queue to be processed. They showed that in the absence of a driving force α can vary between 1/2 and 1 [6]. Huang *et al.* showed that for small networks the power law fails [19]. To compare with the aforementioned results, we also provide the long-time σ - w relations for both the SRW and CRW.

II. MODEL

In our model, RWers, each carrying one unit of information (content), are injected into an undirected network (with \mathcal{N} vertices) through “source” nodes. At a given time, the numbers of RWers entering the network through different source nodes are assumed to be uncorrelated and independent of the content already present in the system. However, these numbers and also the entry points (source nodes) may change with time. Containing no disjointed component, the network is represented by $A(t)$, a generally time-dependent adjacency matrix. To incorporate damping, we take an approach that is similar to that of Bonner *et al.* [20], *i.e.* the content of each RWer is multiplied by a factor of $r < 1$ after each time step (unlike “mortal” RWers [21, 22], the RWers in our model do not die instantly). Therefore, the RWers

* yyu@ncbi.nlm.nih.gov

arriving at node m at time t may not carry the same content. The *total* weight $\mathbf{w}_m(t)$ of node m is defined as the sum of the contents of all RWers arriving at this node at time t . Before diffusing at time $t + 1$, the weight $\mathbf{w}_m(t)$ is equally redistributed between $N_m(t)$ new independent RWers. In other words, the RWers reaching a node first coalesce and then branch to identical RWers each carrying $\frac{\mathbf{w}_m(t)}{N_m(t)}$ unit of information. This aspect of our model is different from that of the branching RW models (widely studied in the mathematical literature [23]) in which the weight is not conserved (i.e. after branching the RWers carry the same weight as the original RWer). This effectively introduces a ‘‘mixing’’ interaction that leads to indistinguishability. The number of packets arriving at node m at time t and those departing at $t + 1$ ($N_m(t)$) may differ. However, if they are set equal and $r = 1$, SRW is recovered. The model reduces to the CRW, if $N_m(t) = 1$, which in turn can be considered as a special case of coalescing-branching RW (CBRW) where $N_m \geq 1$ is independent of both $\mathbf{w}_m(t)$ and t . In our analysis we consider the general case in which $N_m(\mathbf{w}_m(t), t)$ is a function of $\mathbf{w}_m(t)$ and t . At time $t + 1$, the $N_m(\mathbf{w}_m(t), t)$ packets move independently to one of $n_m(t)$ neighbors of node m with probability $1/n_m(t)$.

Let $\mathbf{w}(t)$ be a row vector whose elements are the total weights of the nodes of the network, and $\mathbf{w}_s(t)$ be a row vector representing the injected content into the system at time t . A possible value for $\mathbf{w}(t + 1)$ is then given by:

$$\mathbf{w}(t + 1) = r \mathbf{w}(t)\mathbf{P}(t) + \mathbf{w}_s(t), \quad (1)$$

where $\mathbf{P}(t)$ is a row-stochastic matrix whose average $\langle \mathbf{P}(t) \rangle$, denoted by $P(t)$, is given by $P_{ij}(t) = A_{ij}(t)/n_i(t)$. Equation 1 for the average values can be written as

$$w(t + 1) = r \sum_{\mathbf{w}} \pi_{\mathbf{w}} \mathbf{w}(t) \langle \mathbf{P}(t) \rangle_{\mathbf{w}} + w_s(t),$$

where the sum is over all possible values of $\mathbf{w}(t)$, $\pi_{\mathbf{w}}$ is the probability of the weight vector to be $\mathbf{w}(t)$, $\langle \bullet \rangle_{\mathbf{w}}$ is the average of \bullet provided that the weight vector is $\mathbf{w}(t)$, $w(t) \equiv \langle \mathbf{w}(t) \rangle$, and $w_s(t) \equiv \langle \mathbf{w}_s(t) \rangle = \mathbf{w}_s(t)$. Although in general $\mathbf{P}(t)$ depends on $\mathbf{w}(t)$, it is easy to see that $\langle \mathbf{P}(t) \rangle_{\mathbf{w}} = \langle \mathbf{P}(t) \rangle = P(t)$, and hence

$$w(t + 1) = r w(t)P(t) + w_s(t), \quad (2)$$

Using Eqs. 1 and 2 one finds the following for the covariance matrix $C(t) \equiv \langle \mathbf{w}^T(t)\mathbf{w}(t) \rangle - w(t)^T w(t)$:

$$C(t + 1) = r^2 [P(t)^T C(t) P(t) + X(t)] \quad (3)$$

$$X(t) = \langle \mathbf{P}(t)^T \mathbf{w}(t)^T \mathbf{w}(t) \mathbf{P}(t) \rangle - P(t)^T \langle \mathbf{w}(t)^T \mathbf{w}(t) \rangle P(t),$$

where T denotes transpose. To find $X(t)$, we notice

$$\langle \mathbf{P}_{mi}(t) \mathbf{w}_m(t)^2 \mathbf{P}_{mj}(t) \rangle = \sum_{\mathbf{w}} \pi_{\mathbf{w}} \langle \mathbf{P}_{mi}(t) \mathbf{P}_{mj}(t) \rangle_{\mathbf{w}} \mathbf{w}_m(t)^2.$$

Assuming that node i is connected to node m and that

there are N_m packets present at this node, one can write

$$\langle \mathbf{P}_{mi}^2 \rangle = \sum_{n=1}^{N_m} \mathcal{P}(n) \left(\frac{n}{N_m} \right)^2 = \frac{N_m + n_m - 1}{N_m n_m^2}$$

$$\mathcal{P}(n) = \frac{N_m!}{n!(N_m - n)!} \left(\frac{1}{n_m} \right)^n \left(1 - \frac{1}{n_m} \right)^{N_m - n}$$

where $\mathcal{P}(n)$ is the probability for node i to receive n (out of N_m) packets (dependence on time and $\mathbf{w}_m(t)$ have been omitted for simplicity). Given that node i has received n packets, the average number of packets sent to node $j \neq i$ is $(N_m - n)/(n_m - 1)$, and so

$$\langle \mathbf{P}_{mi} \mathbf{P}_{mj} \rangle = \sum_{n=1}^{N_m} \mathcal{P}(n) \frac{n(N_m - n)}{N_m^2 (n_m - 1)} = \frac{(N_m - 1)}{n_m^2 N_m},$$

provided that nodes i and j are both connected to node m . In other words

$$\langle \mathbf{P}_{mi} \mathbf{P}_{mj} \rangle = \frac{\delta_{ij}}{N_m} P_{mi} + \frac{N_m - 1}{N_m} P_{mi} P_{mj}. \quad (4)$$

Note that when calculating $X(t)$, terms containing $\langle \mathbf{w}_m(t) \mathbf{w}_k(t) \rangle$ cancel out, and hence Eq. 4 can be used to find

$$X(t) = -P(t)^T \text{diag}(v(t)) P(t) + \text{diag}(v(t)P(t)), \quad (5)$$

where $\text{diag}(v(t))$ is a diagonal matrix whose diagonal elements are the components of vector $v(t)$ given by $v_m(t) = \langle \mathbf{w}_m(t)^2 / N_m(\mathbf{w}_m(t), t) \rangle$.

III. RESULTS AND DISCUSSION

Equations 3 and 5 are valid for any RW model that follows Eq. 1 and provide an exact, recursive solution for time-dependent fluctuations in a network with a time-dependent adjacency matrix. However, in the rest of this paper we assume that $\{A_{ij}\}$ are time-independent, and mainly focus on the effect of r on the solutions for the special cases of SRW, CRW and CBRW under special conditions. One should keep in mind that, for given r and w_s , in a time-independent network, $w(t)$ is the same for all RWs that are described by the proposed model, and is given by

$$w(t) = \sum_{n=0}^t w_s(t - n) r^n P^n.$$

However, $\sigma(t)$ (a vector consisting of the node-wise standard deviations) depends on the details of the RW model, i.e. $v(t)$. It should also be noted that both $w(t)$ and $\sigma(t)$ depend on w_s and how it varies with time. For simplicity, here we only consider RWs in which $w_s(t)$ either is a constant or vanishes after $t = 0$ ($w_s(t > 0) = 0$); RWers are injected into the system only at $t = 0$. The latter case ($w_s(t > 0) = 0$) is considered only for undamped SRW

and a special but important case of undamped CRW in which RWers enter the system from all nodes at $t = 0$. In what follows, we first calculate $w(t)$ and $\sigma(t)$ (for some important special cases) in the absence of damping, and then investigate the effect of damping. In each case the long-term σ - w relation is also studied, while the formal asymptotic analyses are provided in the Appendix.

A. Undamped RWs ($r = 1$)

In an undamped RW on a time-independent network, the solution for $w(t)$ is further simplified to $w(t) = \sum_{n=0}^t w_s(t-n)P^n$. If RWers are injected into the network only at $t = 0$, i.e. if $w_s(t > 0) = 0$, we get $w(t) = w_s(0)P^t$. On the other hand, when w_s is constant we have

$$w(t) = w_s \sum_{n=0}^t P^n,$$

which may be rewritten as

$$w(t) = N_{\text{RW}}(w_\infty t + w_1 + w_2),$$

where $N_{\text{RW}} = \sum_i w_{s_i}$ is the number of RWers injected into the system at each time step, $w_1 = \frac{1}{N_{\text{RW}}} w_s \sum_{n=0}^{\infty} (P^n - P^\infty)$ is a constant, and $w_2 = -\frac{1}{N_{\text{RW}}} w_s \sum_{n=t+1}^{\infty} (P^n - P^\infty)$ has a decreasing magnitude with time. Here $P_{ij}^\infty = \frac{n_j}{2E}$ with E being the number of edges in the network. Therefore, when w_s is constant, $w(t \rightarrow \infty) \approx N_{\text{RW}} w_\infty t$, where $w_\infty = \frac{n_i}{2E}$. This expression for $w(t \rightarrow \infty)$ is equivalent to the previously reported formula for SRW (see, for example, [24]). As mentioned before, the solution for $\sigma(t)$ depends on the type of RW. In the following paragraphs we consider a few cases of interest.

1. SRW when $w_s(t > 0) = 0$

With $N_m(t) = \mathbf{w}_m(t)$, a SRW has $v(t) = \langle \mathbf{w}_m(t)^2 / N_m \rangle = w(t)$. Assuming $w_s(t > 0) = 0$ ($w(t) = w_s(0)P^t$) Eq. 3 is simplified to $\tilde{C}(t) = P^T \tilde{C}(t-1)P = P^{t^T} \tilde{C}(0)P^t$, where $\tilde{C}(t) = C(t) - \text{diag}(w(t))$. Therefore,

$$\sigma(\text{SRW}; t)^{(2)} = w(t) - w_s(0)(P^t)^{(2)} = w_s(0)[P^t - (P^t)^{(2)}],$$

where $(\cdot)^{(2)}$ denotes element-wise square and $\sigma(t)^{(2)}$ is a vector consisting of the diagonal elements of $C(t)$ (note that $C(0) = 0$ and that $w(0) = w_s(0)$). If the smallest eigenvalue λ_m of P is not -1 , $P^{t \gg 1}$ approaches P^∞ [15, 24]. However, when $\lambda_m = -1$, $P^{t \gg 1}$ alternates between two matrices whose average converges to P^∞ . Therefore,

$$\sigma(\text{SRW}; t \rightarrow \infty)^{(2)} \approx N_{\text{RW}}(w_\infty - a w_\infty^2),$$

where $a = 1 + \delta_{\lambda_m, -1}$. This result is in agreement with the previously reported long-term σ for SRW (see, for example, [15]).

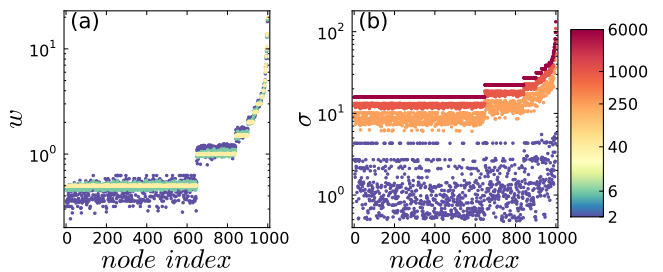


FIG. 1. (Color) Plots of σ and w at different times for all nodes of a scale-free ($\gamma = 3$) [25] with 1000 nodes, traversed by coalescing RWers that have entered the system from all nodes at $t = 0$. The nodes are sorted based on their degrees, i.e. if the index of node i is higher than that of node j , then $n_i \geq n_j$. After a long enough time both w and σ (although with different time scales) converge to values that only depend on the node degrees.

2. SRW with a constant w_s

If the SRWers enter the system at a constant rate and from the same sources, i.e. if w_s is constant, we can add their variances to get

$$\sigma(\text{SRW}; t)^{(2)} = w(t) - w_s \sum_{n=0}^t (P^n)^{(2)}. \quad (6)$$

Since the total number of SRWers at t is $N_{\text{RW}}t$ and the long-time variance for a single SRWer is $w_\infty - a w_\infty^{(2)}$, we get $\sigma^{(2)}(\text{SRW}; t \rightarrow \infty) = N_{\text{RW}}t(w_\infty - a w_\infty^{(2)})$. Hence, if $n_i/2E \ll 1$ (e.g. for typical large networks), we get $\sigma^{(2)}(\text{SRW}; t \rightarrow \infty) \approx w(t \rightarrow \infty)$, which indicates $\alpha \approx 1/2$ for SRW

3. CRW when $w_{s_i} = \delta_{i0}$

In a CRW, lacking a simplified short-term solution similar to Eq. 6, one must use Eq. 3 to find $\sigma(t)$ (Here $N_m = 1$ and $v_m(t) = \langle \mathbf{w}_m(t)^2 \rangle = w_m(t)^2 + \sigma_m(t)^2$). As an example, we consider a special case of CRW in which undamped CRWers are injected from all nodes into a time-independent network at $t = 0$. This example is of special interest because it can be mapped to the extensively studied voter model [10]. However, previous studies focus on calculating the average time for all RWers to coalesce. Our results complement published reports by giving a solution for w and σ . Using a random scale-free network, we solve the time-dependence of w and σ , as shown in Fig. 1. The figure indicates that after a short time, nodes with the same degree do not necessarily have the same w or σ^2 . After a long time, however, nodes with the same degree converge to the same values. This behavior is expected, because all RWers eventually coalesce, after which the model becomes equivalent to a SRW.

4. CBRW with a constant w_s

It can be shown (see the Appendix) that when w_s is constant and for large t , $C(t) = C_\infty t^2 + \mathcal{O}(t)$ for CRW and CBRW. Substituting this asymptotic form into Eqs. 3 and 5 (with $v(t) = (1/N_m)(w_m(t)^2 + \sigma_m(t)^2)$), we find the diagonal elements of C_∞ (called $\sigma_\infty^{(2)}$ (CBRW)) to be (see the Appendix)

$$\sigma_\infty^{(2)}(\text{CBRW}) = (N_{\text{RW}}^2/a)[w_\infty B - a w_\infty^{(2)}], \quad (7)$$

where

$$\begin{aligned} B &= [I + DQ(I - Q)^{-1}]^{-1}, \\ D_{ml} &= \delta_{ml} \frac{N_m - 1}{N_m}, \\ Q &= \sum_{n=0}^{\infty} [P(P^n)^{(2)} - (P^{n+1})^{(2)}], \end{aligned}$$

and I is the identity matrix. Remember that a CRW has $N_m = 1$ (for all m), thus $B = I$ and the result is very similar to that of SRW, albeit the latter grows linearly with time. In addition, if $n_i/2E \ll 1$ (e.g. for typical large networks), SRW has $\sigma^{(2)}(t \rightarrow \infty) \approx w(t \rightarrow \infty)$ while CRW has $\sigma^{(2)}(t \rightarrow \infty) \approx \frac{N_{\text{RW}} t}{a} w(t \rightarrow \infty)$, both indicating that $\alpha \approx 1/2$. Note that one should investigate the relation between σ and $\tilde{w} = w - w_s$ rather than w , because the added RWers at each step ($w_s(t)$) do not diffuse until the next step. However, at this limit $w \approx \tilde{w}$.

In Fig. 2 (a), where log-log plots of σ vs \tilde{w} are shown, we see that the data points corresponding to CRW (top line), and those associated with SRW (bottom line), lie on lines with slopes that are very close to $1/2$ ($\alpha = 0.498$). On these two lines, each point represents a population of nodes with the same degree that also have the same \tilde{w} and σ . For comparison, Fig. 2 (a) also shows the results for the CBRW (where B is not the identity matrix) when branching occurs based on the node degrees (i.e. $N_m = n_m$). In this case, nodes with the same degree do not necessarily have the same σ . Although $\alpha = 0.502$ (when a least-square fitting is applied to the entire data set), the quality of the fit, measured by R^2 , is lower (0.963).

5. Generalized CBRW with a constant w_s

CBRW, which includes CRW as a special case, can be further generalized to incorporate a branching probability q . In such a model, which we call generalized CBRW (GCBRW), the content of node m either branches, with probability q , into $N_m > 1$ packets or moves as one ($N_m = 1$), with probability $1 - q$. It is easy to show that for such a model Eq. 7 is valid if D is replaced by qD . For comparison with CRW ($q = 0$) and CBRW ($q = 1$), the results for $q = 0.5$ are also shown in Fig. 2(a). Interestingly, a much larger spread in σ is observed for GCBRW when $q = 0.5$. Again α remains close to $1/2$ (0.504), although the fit quality is poor ($R^2 = 0.688$), suggesting

that the power law can be fragile upon introduction of coalescing-branching interaction among the RWers.

B. Damped RWs ($r < 1$)

We now discuss the important effect of damping, present in most real-life networks. For example, protein degradations by proteases can be viewed as damping in protein-protein interaction networks [2–4]. Damping also brings out a fundamental difference between GCBRW/CBRW/CRW and SRW: unlike GCBRWers, SRWers are generally distinguishable when $r < 1$. With multiple damped SRWers (dSRWers), Eq. 1 does not hold (although the problem is solvable, see the Appendix). To preserve indistinguishability, the simplest choice is to introduce the coalescing-branching interaction among the RWers in GCBRW or its variants. Here, we compute the long-term (steady state) σ for a GCBRW in which w_s and N_m are time-independent. The steady state has

$$w = w_s \sum_{n=0}^{\infty} r^n P^n = w_s (I - rP)^{-1}.$$

Also, $C(t+1) = C(t) = C$ and $X(t) = X$ are constants, hence Eq. 3 can be solved to get $C = \sum_{n=0}^{\infty} r^{2n+2} P^{nT} X P^n$ or $\sigma^{(2)} = vQ$ (the diagonal values of C), where Q is generalized to incorporate damping, i.e.

$$Q = \sum_{n=0}^{\infty} r^{2n+2} [P(P^n)^{(2)} - (P^{n+1})^{(2)}].$$

Note that for a GCBRW, $v_m(t) = (\sigma^2(t) + w^2(t))K$, where $K = I - qD$. Hence

$$\sigma(\text{GCBRW}; t = \infty)^{(2)} = w^{(2)} [(I - KQ)^{-1} - I]. \quad (8)$$

Equation 8 implies that, unlike the $r = 1$ case, the nodes do not necessarily cluster based on their node degrees. In fact, as shown in Fig. 2 (b), when $r \ll 1$ and with a single source, the nodes are clustered based on their distances from the source, because the RWers taking the shortest path from the source to a given node carry much larger weights than the others. Thus, both node degrees and proximity to the source may contribute to node population formation. As demonstrated in Fig. 2 (c), these two competing effects can significantly change α . The figure indicates that when there is only one source and in a damped ($r \leq 0.95$) scale-free network with 1000 nodes, σ and \tilde{w} can be well fitted ($R^2 > 0.95$) by a power-law relation with $\alpha > 1/2$. Indeed, as larger than $1/2$ have been reported in real-world complex networks [17, 26]. However, $\alpha < 1/2$ can occur depending on the network size (see the Appendix). Interestingly, deviation of α from $1/2$ is significant even when damping is very small (especially for CBRW, i.e. $q = 1$), a phenomenon that is expected to be more pronounced in larger scale-free networks (see the Appendix).

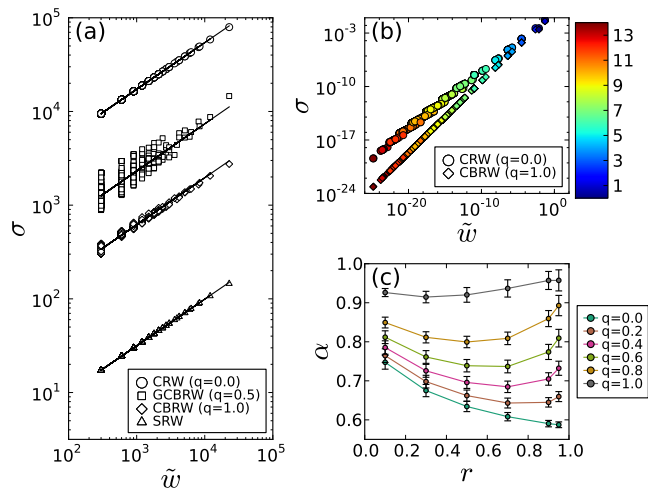


FIG. 2. (Color) (a) Plots of σ vs \tilde{w} , calculated using Eqs. 2, 3 and 5 at $t = 6 \times 10^5$, are shown for a scale-free network with 1000 nodes when $r = 1$. (b) logarithmic σ - \tilde{w} plots are shown for CRW and CBRW with a randomly picked source and when $r = 0.1$. Equation 8 was used to calculate σ . When computing Q , the series was truncated after n terms, where n is the first integer for which $r^n < 10^{-16}$. The nodes are color-coded based on their distances from the source. (c) The average α is plotted as a function of r and for different values of q for a GCBRW, when there is only one source. An α was calculated corresponding to each node (selected as the single source) and the results were averaged. In each case α was computed by a least-square linear fit. The error bars show three times the standard deviations in α .

Evidently, the system parameters such as r , q (if such a probability is introduced in the model), and the number of sources influence how the (\tilde{w}, σ) pairs scatter on the log-log plane, thus determining the goodness of a power-law fit. A complete investigation of how the data distribution, e.g., the shapes of data point clusters and the spread size within each cluster, varies with the system parameters is beyond the scope of the current study, but it definitely deserves to be further investigated.

IV. CONCLUSIONS

In summary, our RW model incorporates three distinguishing features: time-dependence, information loss (damping, $r \leq 1$), and coalescing-branching interactions among RWers. This model is general and includes widely studied SRW and CRW (and its variants CBRW/GCBRW) as special cases. Exact, node-wise solutions are provided for \tilde{w} and σ . For time-independent networks, we also numerically investigate, when $t \gg 1$, whether σ and \tilde{w} are related by a power law. It is shown that in undamped ($r = 1$) GCBRW, although a power-law relation ($\sigma \propto \tilde{w}^\alpha$) can be fitted with $\alpha \approx 1/2$, the quality of fit can be poor for intermediate q values. However, for a single source and when the pervasive damping

effect is considered, the power-law relation becomes robust ($R^2 > 0.95$ for $r \leq 0.95$) with a new twist: the exponent α can easily take a value other than $1/2$.

ACKNOWLEDGEMENTS

This work was supported by the Intramural Research Program of the National Library of Medicine at the National Institutes of Health.

APPENDIX

A. Asymptotic behavior

As shown in the main text, for an undamped system with time-independent w_s and P , we have

$$w(t) = N_{\text{RW}}(w_\infty t + w_1 + \mathcal{O}(t^{-\eta})),$$

where $N_{\text{RW}} = \sum_i w_{s_i}$ is the number of RWers injected into the system at each time step, $w_1 = \frac{1}{N_{\text{RW}}} w_s \sum_{n=0}^{\infty} (P^n - P^\infty)$ does not depend on time, and $\eta > 0$. This solution is valid for any RW model that is described by Eq. 1, including SRW and CBRW.

For the covariance matrix, we assume the asymptotic form

$$C(t) = C_\infty t^\beta + \mathcal{O}(t^\nu) \quad (\nu < \beta),$$

and find β and C_∞ . Note that C_∞ , and any other coefficient in the asymptotic expansion, has the following property $P^{\infty T} C_\infty P^\infty = 0$. To prove this, we observe that for any matrix X , $[P^{\infty T} X P^\infty]_{ij} = (n_i n_j / (2E)^2) \text{sum}(X)$, where $\text{sum}(X)$ denotes the sum of all elements of X . Therefore, for any vector v , $P^{\infty T} [-P^T \text{diag}(v) P + \text{diag}(v P)] P^\infty = P^{\infty T} [\text{diag}(v(P - I))] P^\infty$ vanishes, because $\sum_k v_k = \sum_{k,k'} P_{k'k} v_{k'}$ (recall that $\sum_k P_{k'k} = 1$). Thus, Eq. 3 implies that

$$\begin{aligned} P^{\infty T} C(t+1) P^\infty &= P^{\infty T} C(t) P^\infty \\ &= \dots = P^{\infty T} C(0) P^\infty = 0, \end{aligned} \quad (\text{A1})$$

because $C(0)$ only has zero matrix elements. Hence, any coefficient in the asymptotic expansion of $C(t)$ must also satisfy Eq. A1. In the following subsections we use the asymptotic expansion of $w(t)$, and Eq. A1 to find the asymptotic behavior of $\sigma^{(2)}(t)$ in SRW and CBRW, provided that P and w_s are time-independent.

1. SRW

Since $w(t \rightarrow \infty) = N_{\text{RW}} w_\infty t$, Eq. 6 suggests that, in a SRW and in the limit of large t , the leading term of $\sigma^{(2)}(t)$ grows linearly (or slower) with time. This is because the

second term in Eq. 6 cannot be larger than the first. Therefore, $\beta \leq 1$ and we first attempt the largest possible β value, i.e., $C(t) = C_\infty t + \mathcal{O}(t^\nu)$, where $\nu < 1$. Recall that for a SRW $v(t) = w(t) = N_{\text{RW}}(w_\infty t + w_1 + \mathcal{O}(t^{-\eta}))$. Substituting these values in Eqs. 3 and 5 and keeping the leading terms, we find

$$C_\infty = P^T C_\infty P + N_{\text{RW}}[-P^T \text{diag}(w_\infty)P + \text{diag}(w_\infty P)] \quad (\text{A2})$$

Equation A2 can be iteratively solved to get $C_\infty = N_{\text{RW}} \sum_{n=0}^{\infty} P^{nT} [-P^T \text{diag}(w_\infty)P + \text{diag}(w_\infty P)] P^n$. The diagonal elements of C_∞ are then given by $\sigma_\infty^{(2)} = N_{\text{RW}} w_\infty Q$, where $Q = \sum_{n=0}^{\infty} [P(P^n)^{(2)} - (P^{n+1})^{(2)}]$. Noting that $w_\infty P = w_\infty$ and $w_\infty (P^\infty)^{(2)} = w_\infty^{(2)}$, we find $w_\infty Q = w_\infty - a w_\infty^{(2)}$. Thus

$$\sigma_\infty^{(2)}(\text{SRW}) = N_{\text{RW}}(w_\infty - a w_\infty^{(2)}). \quad (\text{A3})$$

To find the subleading term of $\sigma^{(2)}(t)$, we assume

$$C(t) = C_\infty t + C_1 t^\nu + \mathcal{O}(t^{\nu_0}) \quad (\nu_0 < \nu < 1),$$

and find the largest ν for which C_1 does not vanish. For any $\nu > 0$, substituting $C(t)$ in Eq. 3 and taking the subleading contributions (terms in t^ν) results in $C_1 = P^T C_1 P = P^\infty{}^T C_1 P^\infty = 0$. If $\nu = 0$, however, the same procedure results in

$$C_1 = P^T C_1 P + N_{\text{RW}}[-P^T \text{diag}(w_1)P + \text{diag}(w_1 P)] - C_\infty. \quad (\text{A4})$$

Solving this equation iteratively, we find the following for the diagonal elements of C_1 (denoted by ρ_1)

$$\rho_1 = N_{\text{RW}} w_1 Q - g(C_\infty), \quad (\text{A5})$$

where $g(\bullet) = (\sum_{n=0}^{\infty} P^{nT} \bullet P^n)_{\text{diag}}$, and $(x)_{\text{diag}}$ is a vector comprising the diagonal elements of the matrix x .

2. CBRW

Assuming N_m is also time-independent, we consider the asymptotic form $C(t) = C_\infty t^\beta + \mathcal{O}(t^\nu)$ and find the largest β for which C_∞ is nonzero (here $\nu < \beta$). In a CBRW, $v(t) = (\sigma^{(2)}(t) + w^{(2)}(t))K$ with $K = I - D$, where (as defined in the main text) $D_{lm} = \delta_{lm} \frac{N_m - 1}{N_m}$. Therefore, $v(t)$ takes the asymptotic form of $v(t) = v_\infty t^\mu + \mathcal{O}(t^{\mu_0})$, where $\mu_0 < \mu$, μ is the maximum of 2 and β , and

$$v_\infty = (b_1 \sigma_\infty^{(2)} + b_2 N_{\text{RW}}^2 w_\infty^{(2)})K, \quad (\text{A6})$$

where b_1 and b_2 are either 0 or 1 depending on β : if $\beta < 2$, $b_1 = 0$ and $b_2 = 1$, if $\beta = 2$, $b_1 = b_2 = 1$, and if $\beta > 2$, $b_1 = 1$ and $b_2 = 0$. Note that for the special case of CRW, $K = I$. With the assumption that $\beta \geq 2$, we

substitute $C(t)$ and $v(t)$ in Eqs. 3 and 5 and keep only the leading terms to find

$$C_\infty = P^T C_\infty P - P^T \text{diag}(v_\infty)P + \text{diag}(v_\infty P) \quad (\text{A7})$$

From Eq. A7 we get $C_\infty = \sum_{n=0}^{\infty} P^{nT} [-P^T \text{diag}(v_\infty)P + \text{diag}(v_\infty P)] P^n$ or $\sigma_\infty^{(2)} = v_\infty Q$. If $\beta > 2$, and so $v_\infty = \sigma_\infty^{(2)} K$, we find $\sigma_\infty^{(2)} = 0$, showing that in the asymptotic expansion of $\sigma^{(2)}(t)$ no term with an exponent larger than 2 exists. If $\beta = 2$, $v_\infty = (\sigma_\infty^{(2)} + N_{\text{RW}}^2 w_\infty^{(2)})K$, and we arrive at

$$\sigma_\infty^{(2)} = N_{\text{RW}}^2 w_\infty^{(2)}(F - I) \quad (\text{A8})$$

where $F = [I - KQ]^{-1}$. Equation A8 is the same as Eq. 8 with w replaced by $N_{\text{RW}} w_\infty$. It is easy to see that $F = (I - Q)^{-1} B$, where $B = [I + DQ(I - Q)^{-1}]^{-1}$. Also, note that $w_\infty Q = w_\infty - a w_\infty^{(2)}$ or equivalently $w_\infty^{(2)}(I - Q)^{-1} = (1/a)w_\infty$. Therefore, Eq. A8 can be re-written as Eq. 7.

In a very similar way, one can show that the two subsequent terms in the asymptotic expansion of $C(t)$ are linear and constant in time, i.e.

$$C(t) = C_\infty t^2 + C_1 t + C_2 + \mathcal{O}(t^{-\epsilon}) \quad (\epsilon > 0),$$

and that C_1 and C_2 satisfy the following equations

$$C_1 = P^T C_1 P - P^T \text{diag}(v_1)P + \text{diag}(v_1 P) - 2C_\infty \quad (\text{A9})$$

$$C_2 = P^T C_2 P - P^T \text{diag}(v_2)P + \text{diag}(v_2 P) - (C_\infty + C_1),$$

where v_1 and v_2 are given by

$$v_1 = (\rho_1 + 2N_{\text{RW}}^2 w_\infty * w_1)K \quad (\text{A10})$$

$$v_2 = (\rho_2 + N_{\text{RW}}^2 w_1^{(2)})K,$$

where $*$ denotes element-wise multiplication. Here ρ_1 and ρ_2 are two vectors comprising of the diagonal elements of C_1 and C_2 respectively, i.e.

$$\sigma(t)^{(2)} = \sigma_\infty^{(2)} t^2 + \rho_1 t + \rho_2 + \mathcal{O}(t^{-\epsilon}) \quad (\epsilon > 0).$$

Solving Eqs. A9 one finds

$$\rho_1 = 2N_{\text{RW}}^2 (w_\infty * w_1)(F - I) - 2g(C_\infty)F \quad (\text{A11})$$

$$\rho_2 = N_{\text{RW}}^2 w_1^{(2)}(F - I) - g(C_\infty + C_1)F.$$

It is worth noting that CRW and CBRW can both be regarded as special cases of GCBRW with $q = 0$ and $q = 1$, respectively (q is the branching probability). The matrix K for CRW and CBRW is equal to I and $I - D$ respectively. This suggests that in general for a GCBRW $K = (I - qD)$. Therefore, in the case of a GCBRW, one can use the aforementioned equations to calculate $\sigma_\infty^{(2)}$, ρ_1 and ρ_2 with $K = (I - qD)$.

To compare the approximate solution given here with the exact result obtained from Eq. 3, in Fig. 3 we plot (in red; light gray in the print version) the maximum relative difference between the two solutions, i.e.

$$\Delta = \max[\text{abs}((\sigma_{\alpha_i}^2(t) - \sigma_{\epsilon_i}^2(t))/\sigma_{\epsilon_i}^2(t))],$$

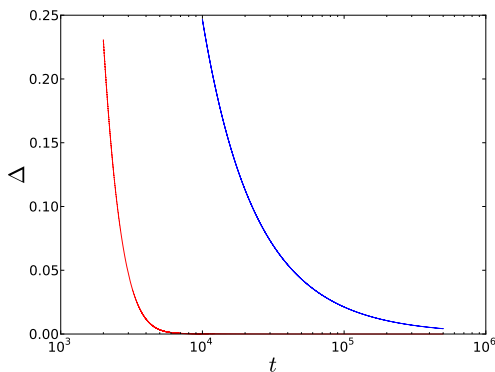


FIG. 3. (Color online) The figure shows the maximum relative difference (as defined in the text) between the exact variances and the approximate values. The red line (light gray in the print version) shows how Δ decreases when the variances are approximated by $\sigma_\infty^{(2)}t^2 + \rho_1t + \rho_2$. When only the leading term ($\sigma_\infty^{(2)}t^2$) is kept, the decrease in Δ is much slower (blue line; dark gray in the print version). However, after a long enough time, the variances are well approximated by the dominant term. The results shown in the figure were computed for the same network used in the main text and for a CBRW. A similar trend is observed for a GCBRW with different q values (data not shown).

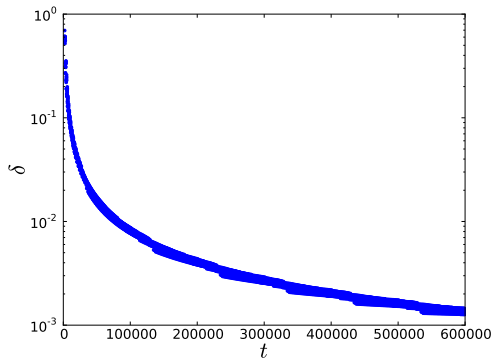


FIG. 4. (Color online) For a scale-free network with 1000 nodes, the maximum relative difference between the variances given by the SRW and CBRW (with the assumptions $N_m(t) = \lceil w_m(t) \rceil$, $r = 1$) is plotted as a function of time.

where $\sigma_{e_i}^{(2)}(t)$ is the exact solution for the variance of the node i at time t , $\sigma_a^{(2)}(t) = \sigma_\infty^{(2)}t^2 + \rho_1t + \rho_2$, \max denotes maximum, and abs denotes absolute value. The figure also shows Δ , in blue (dark gray in the print version), when only the leading term (at large t) is considered, i.e. when $\sigma_a^{(2)}(t) = \sigma_\infty^{(2)}t^2$. As expected, in both cases Δ decreases as a function of time, but a much faster decrease is observed when the constant and the linear terms are also included in the solution. The results indicate that after a large enough time $\sigma^{(2)}(t) = \sigma_\infty^{(2)}t^2$ is indeed a good approximation.

Our results seem to suggest that CBRW differs from

SRW significantly even without damping ($r = 1$). We attribute this difference to the packet branching rule at each node being time-independent. In fact, when N_m is set to increase linearly with time, i.e. $N_m(t) = \lceil w_m(t) \rceil$ (here $\lceil x \rceil$ gives the ceiling of x), at the limit of large t , CBRW captures the key features of SRW: $\sigma_m^2(t \rightarrow \infty)$ grows linearly with t and the leading contribution depends only on node degrees. To verify this, we numerically calculated $\sigma_m^2(t)$ for such a system and for the SRW, and, for each node, computed the relative difference between the two. Figure 4 shows how

$$\delta = \max_m \{ |\sigma_m^2(\text{SRW}; t) - \sigma_m^2(t)| / \sigma_m^2(\text{SRW}; t) \}$$

varies with time, which clearly shows the convergence of the two models in the limit of large t .

It is also of interest to investigate how the average total number of packets N_{tot} scales with time when $N_m(t) = \lceil w_m(t) \rceil$ in comparison with the case of $N_m = n_m$. The results of our numerical calculations, obtained using a randomly picked node as source and shown in Fig. 5, indicate that when $N_m = n_m$ is time-independent, N_{tot} converges to a constant (Fig. 5 (a)). On the other hand, the figure indicates when $N_m(t) = \lceil w_m(t) \rceil$, N_{tot} , with a good approximation, increases linearly with time (Fig. 5 (b)). Note that the constant to which N_{tot} converges, when $N_m = n_m$, and the slope of the line, when $N_m(t) = \lceil w_m(t) \rceil$, are generally dependent on the number of sources.

B. Size-dependence of the effect of small damping

In most cases even a small damping significantly changes the power α when a single source is present. To investigate how this effect is dependent on the size of the network, in Fig. 6 (a) we plot the average α as a function of the number of nodes \mathcal{N} for CRW ($q = 0$), CBRW ($q = 1$) and GCBRW with $q = 0.5$, when $r = 0.99$. For each \mathcal{N} , the power α was averaged over all nodes of 100 scale-free networks with \mathcal{N} nodes. For CBRW and GCBRW (with $q = 0.5$), the figure shows a significant deviation from $\alpha = 1/2$ for all studied networks. In the case of a CRW the deviations are smaller, but still significant for larger networks. The figure clearly indicates that damping, even if very small, becomes more and more important in larger networks. The average R^2 s are shown in Fig. 6 (b).

C. Damped SRW

Although a network traversed by multiple damped SRWers (dSRWers) is not described by Eq. 1 (because the RWers are distinguishable), we can still find $\sigma^{(2)}(t)$ for such a system. Since the variance of a dSRWer after t steps is just r^{2t} multiplied by that of a SRWer at time t , the following can be written for a dSRW, provided that

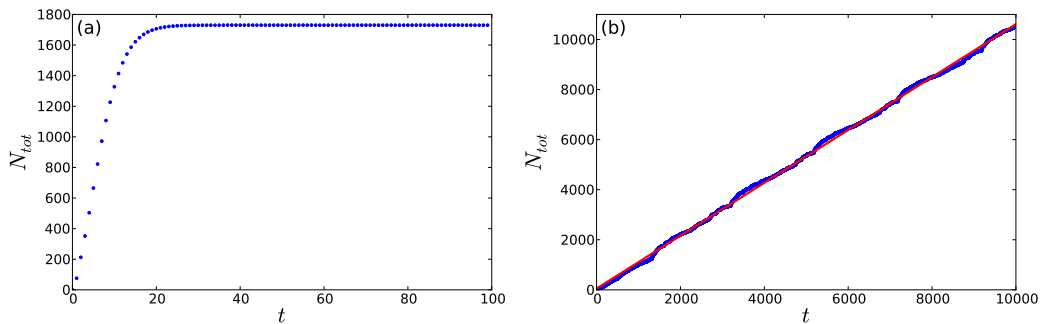


FIG. 5. (Color online) For a scale-free network with 1000 nodes, the average total number of packets N_{tot} is plotted as a function of time when (a) $N_m = n_m$ and (b) $N_m(t) = [w_m(t)]$. A random node was chosen as the source. When the data shown in (b) are fitted by a straight line (red; light gray in the print version), the slope is 1.06 with R^2 being 0.999.

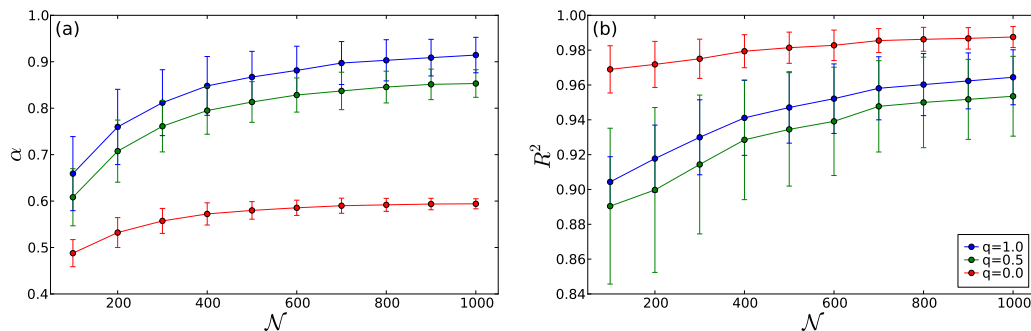


FIG. 6. (Color online) (a) The average α is plotted vs the number of the nodes in the network \mathcal{N} , when damping is very small ($r = 0.99$). The error bars represent the standard deviations of α . The top, middle and bottom lines correspond to $q = 1$, $q = 0.5$, and $q = 0$ respectively. (b) The average R^2 is shown. The error bars are the standard deviations of R^2 . The top, middle and bottom lines correspond to $q = 0$, $q = 1$, and $q = 0.5$ respectively.

P and w_s are constant

$$\sigma^{(2)}(\text{dSRW}; t) = w_s \sum_{n=0}^t r^{2n} [P^n - (P^n)^{(2)}]. \quad (\text{A12})$$

-
- [1] K. I. Goh, M. E. Cusick, D. Valle, B. Childs, M. Vidal, and A. L. Barabasi, Proc. Natl. Acad. Sci. U.S.A. **104**, 8685 (2007).
- [2] A. Stojmirovic and Y.-K. Yu, J. Comput. Biol. **14**, 1115 (2007).
- [3] A. Stojmirovic and Y. K. Yu, J. Comput. Biol. **19**, 379 (2012).
- [4] M. B. Hamaneh and Y.-K. Yu, PLOS ONE **9**, e110936 (2014).
- [5] Z. Eisler and J. Kertesz, Phys Rev E Stat Nonlin Soft Matter Phys **73**, 046109 (2006).
- [6] J. Duch and A. Arenas, Phys. Rev. Lett. **96**, 218702 (2006).
- [7] R. Guimera, A. Diaz-Guilera, F. Vega-Redondo, A. Cabrales, and A. Arenas, Phys. Rev. Lett. **89**, 248701 (2002).
- [8] M. Argollo de Menezes and A. L. Barabasi, Phys. Rev. Lett. **93**, 068701 (2004).
- [9] C. Castellano, S. Fortunato, and V. Loreto, Rev. Mod. Phys. **81**, 591 (2009).
- [10] T. Liggett, *Interacting Particle Systems* (Springer, New York, 1985).
- [11] P. Clifford and A. Sudbury, Biometrika **60**, 581 (1973).
- [12] D. J. Balding and N. J. Green, Phys. Rev., A **40**, 4585 (1989).
- [13] D. Acemoglu, G. Como, F. Fagnani, and A. Ozdaglar, Math Oper Res **38**, 1 (2012).
- [14] K. S. Korolev, M. Avlund, O. Hallatschek, and D. Nelson, Rev Mod Phys **82**, 1691 (2010).
- [15] V. Kishore, M. S. Santhanam, and R. E. Amritkar, Phys. Rev. Lett. **106**, 188701 (2011).
- [16] Y. Z. Chen, Z. G. Huang, and Y. C. Lai, Sci Rep **4**, 6121 (2014).
- [17] S. Meloni, J. Gomez-Gardenes, V. Latora, and Y. Moreno, Phys. Rev. Lett. **100**, 208701 (2008).

- [18] Z. Eisler and J. Kertesz, Phys Rev E Stat Nonlin Soft Matter Phys **71**, 057104 (2005).
- [19] Z. G. Huang, J. Q. Dong, L. Huang, and Y. C. Lai, Sci Rep **4**, 6787 (2014).
- [20] R. F. Bonner, R. Nossal, S. Havlin, and G. H. Weiss, J Opt Soc Am A **4**, 423 (1987).
- [21] S. B. Yuste, E. Abad, and K. Lindenberg, Phys. Rev. Lett. **110**, 220603 (2013).
- [22] E. Abad, S. B. Yuste, and K. Lindenberg, Phys Rev E Stat Nonlin Soft Matter Phys **88**, 062110 (2013).
- [23] S. Asmussen and N. Kaplan, Stoch Proc Appl **4**, 1 (1976).
- [24] J. D. Noh and H. Rieger, Phys. Rev. Lett. **92**, 118701 (2004).
- [25] A. L. Barabasi and R. Albert, Science **286**, 509 (1999).
- [26] A. Fronczak and P. Fronczak, Phys Rev E Stat Nonlin Soft Matter Phys **81**, 066112 (2010).